J Mater Sci: Mater Med (2015) 26:268
DOI 10.1007/s10856-015-5603-3

Original Research

In vitro antimicrobial activity of ZnO based glass–ceramics against pathogenic bacteria

Madeeha Riaz[1] · Rehana Zia[1] · Farhat Saleemi[2] · Hafeez Ikram[1] · Farooq Bashir[1]

Received: 23 March 2015 / Accepted: 19 October 2015 / Published online: 27 October 2015

Abstract The antibacterial activity of ZnO (0–15.53 mol%) based SiO_2–CaO–P_2O_5–Na_2O–CaF_2 bioactive glass–ceramics synthesized by controlled crystallisation were studied against eight micro-organisms using modified Kirby Bauer method. The antibacterial activity of the specimens was statistically evaluated using one-way analysis of variance and $P < 0.05$ was used as the level of significance. In vitro dissolution tests were performed in stimulated body fluid for 48 h at 37 °C for different time intervals to correlate the dissolution behaviour of test samples with antibacterial effects. The results illustrate that specimen BZn15.53 having the highest concentration of ZnO (15.53 mol %) demonstrated the strongest effect against *Staph.aureus, S. epidermidis*, *B. subtilis* and *K. pneumonia*. The effectiveness of BZn15.53 in inhibiting bacteria was due to accumulation of Zn^{+2} ions around the surface of the bacteria cell release that caused the death of the cell, besides the presence of hydroxyapatite phase was also responsible for damaging the cell membrane of bacteria.

1 Introduction

For the last 40 years, biomaterials have been used to replace damaged tissue and improve organ function. The two essential requirements for implants are; that it forms a biological bond with surrounding tissue and without any bacterial infection. Glasses, ceramics and glass–ceramics are particularly good choices as a biomaterial, on account of its biocompatibility, bioactivity, and non-toxic properties, but inspite of all precautionary measures and post-operative hygiene protocol used still 2–4 % chances of bacterial infections persists [1]. Infections caused by bacteria colonization are the most common reasons for failure of implants in bone and tissue engineering [2]. According to Anthony Gristina [3] it is "race for the surface" between tissue cell integration and bacterial adhesion, compete each other to take control over implant surface, host tissue defend the implant surface from invading pathogenic bacteria, but still some bacteria manage to escape the host defense system and show such a high resistant behavior to antibiotics that all remedies failed to rescue the functionality of biomaterial implant. To lessen the potential risks of bacterial colonization much effort has been made; the addition of a special antibacterial agent like silver or implants loaded with antibiotics to resist against infection caused by bacteria, but they hinder the bioactive properties of implant [2, 4–7]. So, there is a need to develop such implants that have the intrinsic property to inhibit bacterial growth without altering the biocompatibilty of the artificial implant. It is believed that antibacterial properties of a material vary with composition, concentration, particle size of antimicrobial agents and microorganisms tested [8]. The antibacterial properties of bioactive materials are observed to be strongly influenced by changes in pH of the supernant [9, 10]. It has been reported that in recent years, incorporation of certain inorganic antimicrobial agents like Ti, B, Ag, Cu, Fe and Zn ions into calcium phosphate structure, not only improves crystallinity, but also improves their antimicrobial property [11–14].

Some ceramics, such as Bioglass® [15], A-W glass–ceramic [16] and hydroxyapatite [17], are most widely used

✉ Madeeha Riaz
madeehariaz2762@yahoo.com

[1] Department of Physics, Lahore College for Women University, Lahore, Pakistan

[2] Government College for Women University, Sialkot, Pakistan

biomaterials because of their ability to form bond with living bone via formation of bone-like apatite layer on its surface [18, 19]. Among these biomaterials, A-W glass–ceramic is very useful material because it exhibits better mechanical properties and strong bone-bonding ability [20] as it is chemically stable, doesn't resolve easily in physiological fluids; which make it attractive for orthopedic and dental applications [21].

In present study zinc oxide is added to apatite-wollastonite glass–ceramic, since zinc oxide is an essential trace element known to improve the bone bonding ability of bio-implant as it stimulates osteoblast adhesion and alkaline phosphatase activity of bone cells [22, 23]. Another significant feature of zinc oxide is its potent chemical and physical stability, in our previous study [24] which is a part of the present study featuring in vitro bioactivity of ZnO (0–15.53 mol%) doped SiO_2–CaO–P_2O_5–Na_2O–CaF_2 it had been reported that addition of ZnO enhanced the chemical durability of the material without affecting much the bioactive properties, which is a beneficial feature for all bioactive materials because if dissolution rate is too high it will produce high concentration of ions which is not effective, and if it is too low than cellular proliferation will be impossible to stimulate due to low ionic concentrations. So, it is very important to control the dissolution rates of implant [25, 26]. Furthermore, the antimicrobial activity associated with Zn ion is regarded as an additional benefit to clinically implanted biomaterials [27, 28]. ZnO nanoparticles have been reported to possess a wide spectrum of antibacterial activities. It has been reported previously that it inhibits the growth of *S.enterica serovar Enteritidiss*, *E. coli* O157:H7, *B. subtilis*, *L. monocytogenes*, *Staph. Saureus*, *Staph. Epidermidis*, *Strept. Pyogenes*, *E. Faecalis* and *C. Jejuni* [29–31]. Earlier much of the work had been done on inorganic antimicrobial agents, which was mostly of pharmaceutical use, but antimicrobial properties of crystalline bioactive implants have not been adequately studied. Recognizing the importance of high risk for biomaterials-related infections there is a need to develop such bio-implants that are biocompatible and have inherent ability to resist these implant associated bacterial infections. The present study aim at evaluating the in vitro antimicrobial action of apatite-wollastonite based glass–ceramic in the SiO_2–CaO–P_2O_5–Na_2O–CaF_2 system doped with different ZnO content against common pathogenic bacteria that are the most common cause of implant failure.

2 Materials and methods

Five different bioactive glasses $(38.73)SiO_2.(49.96)CaO.(6.53)P_2O_5.(x)ZnO.(4.35)Na_2O.(0.43)CaF_2$ (x = 0, 0.76, 3.96, 7.78, 15.53 mol%) were prepared by melt-quenching technique, using chemically pure (99.9 %) silicon dioxide (SiO_2; Merck), calcium oxide ($CaCO_3$; Merck), sodium carbonate (Na_2CO_3; Merck), phosphorous(V)oxide (P_2O_5; Merck), calcium fluoride (CaF_2, Fluka) and zinc oxide (ZnO; RDH), at 1450 °C temperature (chemical composition shown in Table 1 below).

Table 1 The chemical composition (mol%) of prepared glass–ceramics

Sample id	SiO_2	CaO	P_2O_5	CaF_2	Na_2O	ZnO
BZn0	38.73	49.96	6.53	0.43	4.35	0
BZn0.76	38.73	49.20	6.53	0.43	4.35	0.76
BZn3.63	38.73	46.33	6.53	0.43	4.35	3.63
BZn7.78	38.73	42.18	6.53	0.43	4.35	7.78
BZn15.53	38.73	34.43	6.53	0.43	4.35	15.53

Table 2 Glass transition temperature T_g and crystallisation temperature T_c

Sample ID	Glass transition temperature (T_g) °C	Crystallisation temperature (T_{c1}) °C	Crystallisation temperature (T_{c2}) °C
BZn0	700	856	910
BZn0.76	682	847	917
BZn3.63	672	815	897
BZn7.78	661	–	785
BZn15.53	614	–	746

The thermal characterization of the glass powders was studied by Differential Scanning Calorimetry analyzer (SDT-Q600) at heating rate 15 °C/min from room temperature (23 °C) to 950 °C using alumina as reference material. The glass frits were annealed at onset glass transition temperature 'T_g' given in Table 2; for 2 h at a heating rate of 5 °C/min, then pulverized and sieved to a particle size less than 40 μm using agate mortar. Compacts of glass powders having a diameter of 15 mm and thickness of 3 mm were prepared under hydrostatic pressure of 45 MPa. The compacts were sintered for 4 h at crystallization temperature 'T_{c2}′ (given in Table 2 below), obtained from DSC curves (shown in Fig. 1), maintaining 15 ° C/min heating rate and cooled to room temperature initially at slow rate 5 °C/min in order to avoid thermal shock and thereafter at 25 °C/min rate in order to acquire the desired phase. The compacts were again pulverized and sieved to a particle size less than 40 μm using agate mortar for characterization. The crystalline phases produced as a result of heat treatment in fine pulverised samples (40 μm) were identified by Bruker D-8 Discover diffractometer in 18–45° 2θ range using the Ni filter and Cu Kα radiations run at 40 kV and 25 mA. For the interpretation of XRD patterns the JCPDS—International Centre for Diffraction

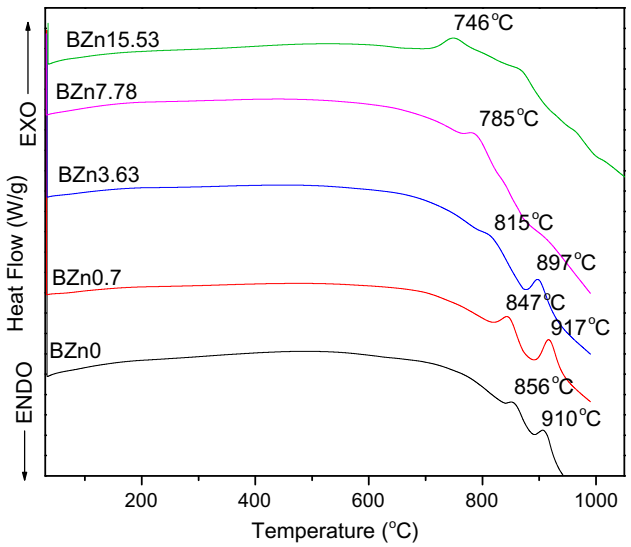

Fig. 1 The DSC thermogram of zinc based glass–ceramics showing crystallisation temperature T_c

Data Cards was used as a reference data. The Antibacterial activity of glass–ceramics were evaluated against eight bacteria and Roxithromycin (0.3 mg) was used as positive control. The bacteria cultivation tests were performed in the Microbiology Laboratory of Pharmacy Department (LCWU, Lahore-Pakistan). The microorganisms used in this study were procured in the Pathology Department of Post Graduate Medical Institute (PGMI), Lahore and are enlisted in Table 3. Modified Kirby Bauer method [32] was used to evaluate the antibacterial activity qualitatively. In this method first cultures of organisms were sub-cultured overnight in Nutrient broth (Merck, Germany) at 35 ± 2 °C then diluted 1/100 in sterile water. The Nutrient Agar (Merck, Germany) solidified on sterilized Petri plates were used as a growth medium for bacterial culture. The bacteria was inoculated on Nutrient Agar (Merck, Germany) medium by swabbing uniformly over the surface of the plate with sterile cotton-tipped swab containing approximately 10^5 colony forming units (CFUs)/ml of bacteria enumerated from images of plates using OpenCFU (3.9.0) software, 20 mg of fine powdered glass–ceramics samples (40 μm) were placed at the centre of each plate before overnight incubation of plates at 35 ± 2 °C. After incubation the antibacterial activity of samples was determined by measuring zone of inhibition (ZI) using vernier calliper (having least count 0.001 mm) to the nearest millimeter. The antibacterial activity test was performed in triplicate. Origin Pro 8 software was used for statistical analysis. By applying one-way analysis of variance (ANOVA) the mean activity of samples was compared and $P < 0.05$ was used as the level of significance. Factors responsible for the antibacterial ability of the specimens were determined by comparing changes in the stimulated body fluid (SBF) prepared according to the method reported by Kokubo and Takadama [33] during immersion of the powdered glass–ceramics with their response to bacteria. After soaking the samples (20 mg) in 10 ml of SBF at 37 °C having pH 7.4 for 1, 2, 4, 8, 24, 32, 48 h the changes in concentration of Si, Ca, Zn, P, Na elements in solution after removing the powder by 0.45 μm filter, were measured by Atomic Absorption Spectrometer (Z-5000, Polarized Zeeman Atomic Absorption Spectrophotometer, Hitachi) and pH values in the bulk filtered solutions after each immersion time. The buffering capacity of SBF, Nutrient broth (NB) and pure water were determined by titration with 0.5 M NaOH. This was achieved by measuring variations in pH level after subsequent additions of 0.1 ml volume of 0.5 M NaOH in 100 ml of medium solution and titaration curves was compared.

3 Results and discussion

3.1 Thermal analysis

The addition of ZnO in the system decreased both glass transition 'T_g' and crystallization temperatures 'T_c' (mentioned in Table 2), thus viscosity of glass decreased which therefore increased the mobility of ions. The DSC result for BZn0, BZn0.76 and BZn3.63 show (Fig. 1) two exothermic peaks correspond to two crystallisation temperatures 'T_{c1}' and 'T_{c2}', the first T_{c1} is correlated to Hydroxyapatite phase while T_{c2} correlated to Wollastonite phase as confirmed by XRD (data not included). It was seen that the induction of ZnO content ≥3.63 mol% in the system at expense of CaO caused broadening of exothermic peaks which may be due to overlapping of peaks.

The exothermic peaks shifted into a single broad peak with further addition of ZnO (>3.63) in the system. No sharp exothermic effect was seen for BZn7.76 and BZn15.53 glass in the DSC curves, it means that the amount of crystalline phases developed during DSC run was small, which is in agreement with XRD analysis shown in Fig. 2. Secondly, it is evident from DSC results of BZn7.76 and BZn15.53 glass that the addition of ZnO concentration >3.63 mol% caused a progressive inhibition of the second thermal event confirmed by a reduction in intensity of wollastonite peaks from XRD analysis (Fig. 2) this result is attributed to replacement of Ca with ZnO, since Zn like Ca has valance charge '+2', hence its replacement makes new interconnections within the silicate network structure.

3.2 Structural analysis

The Powder X-ray Diffraction results are shown in Fig. 2. The XRD of un-doped glass–ceramic identified two

Table 3 The Diameter of Zone of inhibition produced by different SiO_2–CaO–P_2O_5–ZnO–Na_2O–CaF_2 glass–ceramics against gram-positive and gram-negative bacteria

	Sample	Mean (mm)	Standard deviation (SD)	SE of mean	Positive control *Roxithromycin* (mean ± SD)
S. aureus	BZn0	22.7	1.26	0.73	18.7 ± 0.34
	BZn0.76	16.2	0.38	0.22	
	BZn3.63	9.4	0.30	0.17	
	BZn7.78	19.1	0.28	0.16	
	BZn15.53	36.1	0.36	0.21	
S. pyogenes	BZn0	68.0	0.22	0.12	17.3 ± 0.251
	BZn0.76	0	0	0	
	BZn3.63	0	0	0	
	BZn7.78	20.2	0.29	0.17	
	BZn15.53	60.1	0.61	0.35	
S. epidermidis	BZn0	21.3	0.53	0.31	7.6 ± 0.428
	BZn0.76	0	0	0	
	BZn3.63	0	0	0	
	BZn7.78	0	0	0	
	BZn15.53	21.7	0.39	0.22	
B. subtilis	BZn0	0	0	0	9.1 ± 0.231
	BZn0.76	0	0	0	
	BZn3.63	0	0	0	
	BZn7.78	0	0	0	
	BZn15.53	12	0.15	0.09	
K. pneumonia	BZn0	0	0	0	3.5 ± 0.4560
	BZn0.76	0	0	0	
	BZn3.63	0	0	0	
	BZn7.78	0	0	0	
	BZn15.53	11.9	0.06	0.03	
E. coli	BZn0	0	0	0	14.2 ± 0.273
	BZn0.76	0	0	0	
	BZn3.63	0	0	0	
	BZn7.78	0	0	0	
	BZn15.53	0	0	0	
P. mirabilis	BZn0	0	0	0	3.9 ± 0.1562
	BZn0.76	0	0	0	
	BZn3.63	0	0	0	
	BZn7.78	0	0	0	
	BZn15.53	0	0	0	
P. aeruginosa	BZn0	0	0	0	2.4 ± 0.3265
	BZn0.76	0	0	0	
	BZn3.63	0	0	0	
	BZn7.78	0	0	0	
	BZn15.53	0	0	0	

crystalline phases of wollastonite with peaks at 28.94° and 29.72°, and hydroxyapatite with peaks at 31.74°, 21.75° and 32.88° respectively. With the addition of 0.76 % ZnO the peak intensity of the wollastonite phase at 28.94° and 29.72° increased while the peak intensity of the hydroxyapatite phase at 32.88° decreased, whereas, the intensities of hydroxyapatite phase peaks at 31.74 ° and 21.75° remain unchanged. The addition of 3.63 % of ZnO caused a new sharp wollastonite peak appeared at 29.98° and other wollastonite peak present at 29.72° disappeared

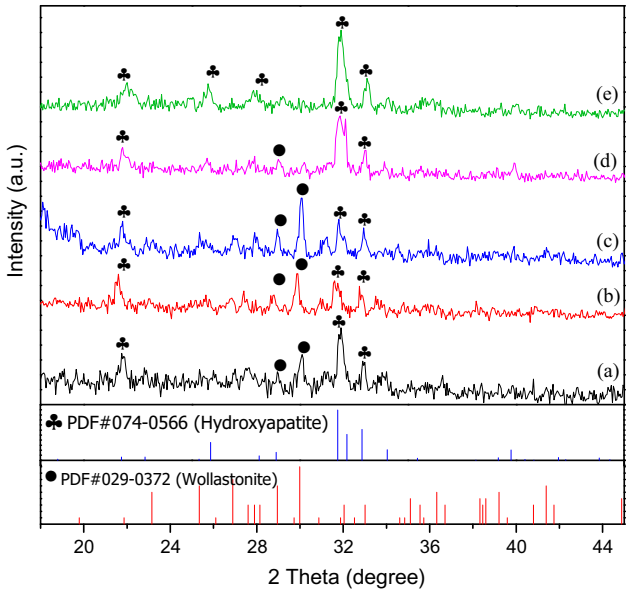

Fig. 2 X-ray diffraction pattern of all glass–ceramics *a* BZn0, *b* BZn0.76, *c* BZn3.63, *d* BZn7.78 and *e* BZn15.53

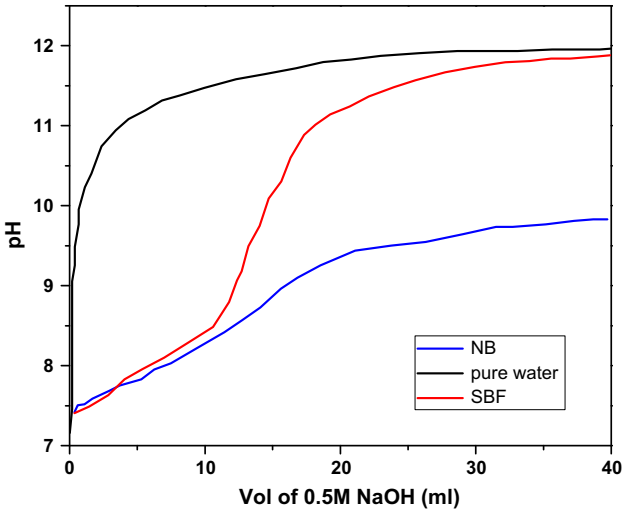

Fig. 3 Titration curves of SBF, NB and pure water titrated with 0.5 M NaOH

while the hydroxyapatite phase peaks remained unchanged. The addition of 7.78 % of ZnO decomposed the wollastonite phase largely, only a small peak at 28.94° was observed while the peak intensity of hydroxyapatite phase at 31.74° increased and peaks at 32.88° and 21.75° remained unchanged, and with 15.53 % ZnO addition wollastonite phase completely disappeared only a single phase of hydroxyapatite was observed for BZn15.53 glass–ceramic, two new hydroxyapatite crystalline peaks at 25.87° and 28.12° appeared and increase in intensity of peaks at 21.75°, 31.74° and 32.88° was also observed. It can be attributed from XRD results that the addition of ZnO ≥7.78 % to the SiO_2–CaO–P_2O_5–Na_2O–CaF_2 glass–ceramic system decomposed the wollastonite phase largely and had pronounced influence on growth of hydroxyapatite phase which is known to be good inhibitor of bacterial colonization [34]. This decrease in peak intensities of wollastonite phase were due to replacement of Ca^{+2} ions with Zn^{+2} ions in the system, as mobility of ions were also largely increased with >7.78 % ZnO addition which caused breakage of bond with Ca^{+2} and Si-O-Si, the presence of hydrogen that form hydroxide group in the system caused reduction in electrostatic interaction between Ca and glass matrix and increased the mobility of Ca ion which subsequently made new connections in the network by joining OH^- and P^- ions resulting increased intensity of Hydroxyapatite phase peaks. No apparent peak shifts was observed and it may be assumed that ZnO remained in the glassy phase as no separate crystalline phase was formed.

3.3 Comparision of buffering capacity

The buffering capacity of SBF used for glass dissolution assays and NB used for bacterial cultivation were compared by titration curves (Fig. 3). The SBF and NB showed similar buffering capacities in the pH range 7.4–8.5 which indicate that pH trends observed in the dissolution studies of powdered samples in SBF were comparable with the pH changes in NB during the antibacterial activity tests.

3.4 Dissolution behaviour

The changes in pH value and concentration of Si, Ca, Na, P and Zn in SBF solution as a function of different immersion time intervals are shown in Figs. 4 and 5 respectively. All the glass–ceramic samples showed similar trend i.e. a rapid increase in pH for first four hours due to ion exchange between the protons H^+ in the solution and alkaline cations (Ca^{2+}, Na^+) present in the glass–ceramics which indicate the formation of silanol (Si–OH) group thereafter the increase in pH slow down, as increase in ionic activity makes the solution supersaturated and this reduced the dissolution rate.

It was observed that with Zn (max conc) ranges from 0 to 0.0046 mol/m^3, the maximum pH value decreased from 8.12 to 7.95, Si (max conc) from 1.65 to 0.95 mol/m^3, Ca (max conc) from 1.66 to 1.32 mol/m^3, Na (max conc) from 10.11 to 8 mol/m^3 while P (max conc) 0.25 to 0.28 after 48 h, which is indicative of reduction in dissolution rate due to addition of ZnO 0 to 15.53 % in the system. The increase in concentration of Si and Ca and decrease in concentration of P from the SBF solution are indicative of surface chemical reaction caused by apatite formation

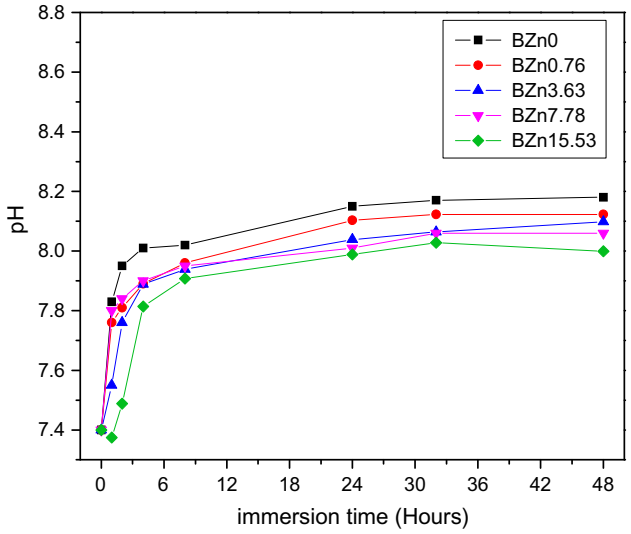

Fig. 4 pH in bulk solution of each glass-ceramic as a function of immersion time

process. The concentration of Zn leached out was strongly correlated with basic concentration of oxide in composition, the amount of Zn concentration leached out in SBF increased with increase in ZnO content in base system.

3.5 Antibacterial activity: a statistical analysis

In vitro antibacterial activity of specimens was examined against eight bacterial strains (given in Table 3) by measuring Diameter of Zone of Inhibition (ZI) (shown in Figs. 6 and 7). Measuring the ZI is considered to be the foremost, fast and inexpensive way [35] to estimate the resistivity of particular test specimen against bacterial growth. The antibacterial test was performed in triplicate and the diameter of ZI measured for each glass–ceramics expressed mean (mm) along with standard derivative and standard error (SE) evaluated by origin pro 8 software is given in Table 3. The antibacterial properties of a biocompatible material were derived from pH value, ionic species of material and type of microorganism [8, 9]. The results showed that these glass–ceramics displayed statistically significant ($P < 0.05$) antimicrobial activity against Gram positive bacteria; *Staph. aureus*, *Strep. Pyogenes, Staph. epidermidis*, *B. subtilis*: and a Gram negative bacteria *Klebsiella pneumonia*.

The un-doped glass–ceramic (BZn0) showed slightly larger and significant inhibition zone against *Strep. pyogenes* ($P < 0.05$) 68.01 ± 0.22 mm, this result may be attributed to high value of pH as compared to others (as the dissolution rate was decreased with ZnO addition which therefore reduced the pH level). Previous studies reported that the antibacterial effect results from one of the surface reactions, that glass derivatives undergo which cause an increase in pH level during leaching and dissolution processes [9]. According to Stoor et al. (1998 and 1999) [36, 37] and Zehnder et al. (2006) [38] increase in concentration of some specific ions like Ca^{+2} and Si^{+2} influence antibacterial activity by inducing hyper-osmotic environment due to high ionic strength of these ions that result in inhibition of bacterial viability. The BZn15.53 showed statistically significant ($P < 0.05$) more potent effect on the studied microorganisms i.e. *Staph.aureus*, *Staph. epidermidis, B. subtilis* and *Klebsiella pneumonia* as compared to others.

To specify the significance level, pair-wise multiple mean comparison (at $P < 0.05$ level of significance) was performed using one-way ANOVA (tabulated in Table 4), all test specimens showed significantly different means against *Staph. aureus* bacteria. The results of the statistical study showed that BZn15.53 demonstrated strongest inhibitory effect against *Staph.aureus, S. epidermidis*, *B. subtilis* and *K. pneumonia bacterial strains*; with inhibition zone (mean $\pm$ SD) 36.07 ± 0.36 mm ($P = 3.41206 \times 10^{-5}$), 21.75 ± 0.39 mm ($P = 3.57448 \times 10^{-6}$), 12 ± 0.15 mm ($P = 3.57448 \times 10^{-6}$) and 11.89 ± 0.06 mm ($P = 8.72391 \times 10^{-6}$) respectively. The evaluation of the results reflects the effectiveness of the BZn15.53 in inhibiting *Staph.aureus, S. epidermidis*, *B. subtilis* and *K. pneumonia* common pathogenic bacteria, this result may be explained by the fact that BZn15.53 contains a high concentration of ZnO which is known to have potent antibacterial ability [39]. The Zn^{+2} ions released from the atomic lattice into the medium are rapidly attracted by the negatively charged phosphate and a carboxylic group of nucleic acids present on the surface of the bacteria, an unspecific CorA MIT transport system is responsible for the fast accumulation of Zn^{+2} ions on the surface of the bacteria which subsequently inhibit endogenous respiration of cells [40]. In addition to that, BZn15.53 specimen had a single phase of hydroxyapatite, Deepa et al. [34] reported significant antibacterial activity of hydroxyapatite. Hydroxyapatite previously regarded as a hydrated oxide of calcium when interact with the cell membrane of bacteria, it caused induction of several reactive oxygen species among them hydrogen peroxide (H_2O_2) considered as a strong oxidizing agent which proved to be lethal to bacterial cells hence responsible for death of bacteria [41]. It was also observed that specimens had a more pronounced effect on Gram-positive bacteria than Gram-negative bacteria. The Gram-negative bacteria less sensitivity to test samples possibly as a result of protein cell wall that provides a permeability barrier to the antibacterial agent (Adwan et al.) [42].

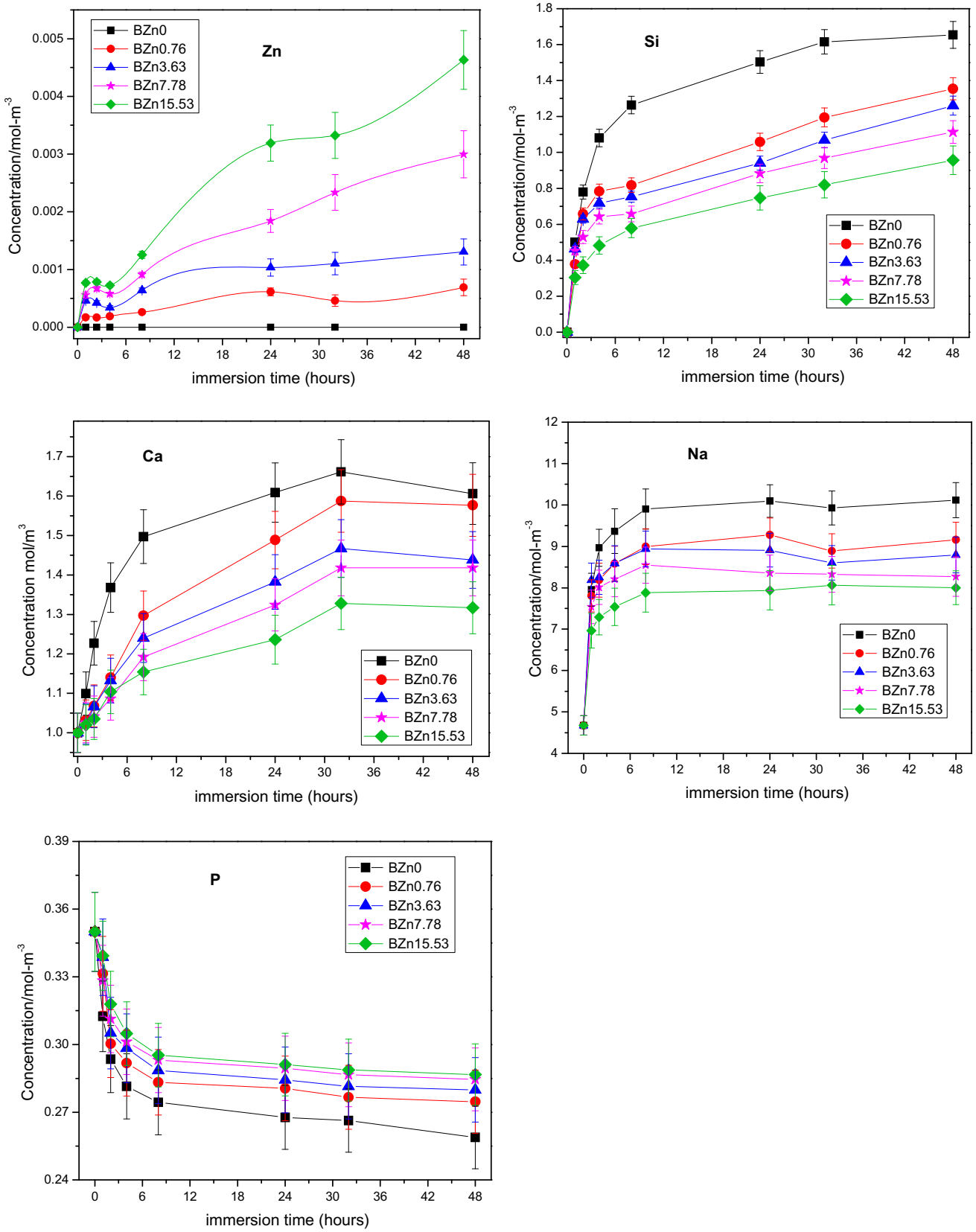

Fig. 5 Variation in pH of solution and concentration of Zn, Si, Ca, Na and P, measured for different soaking time

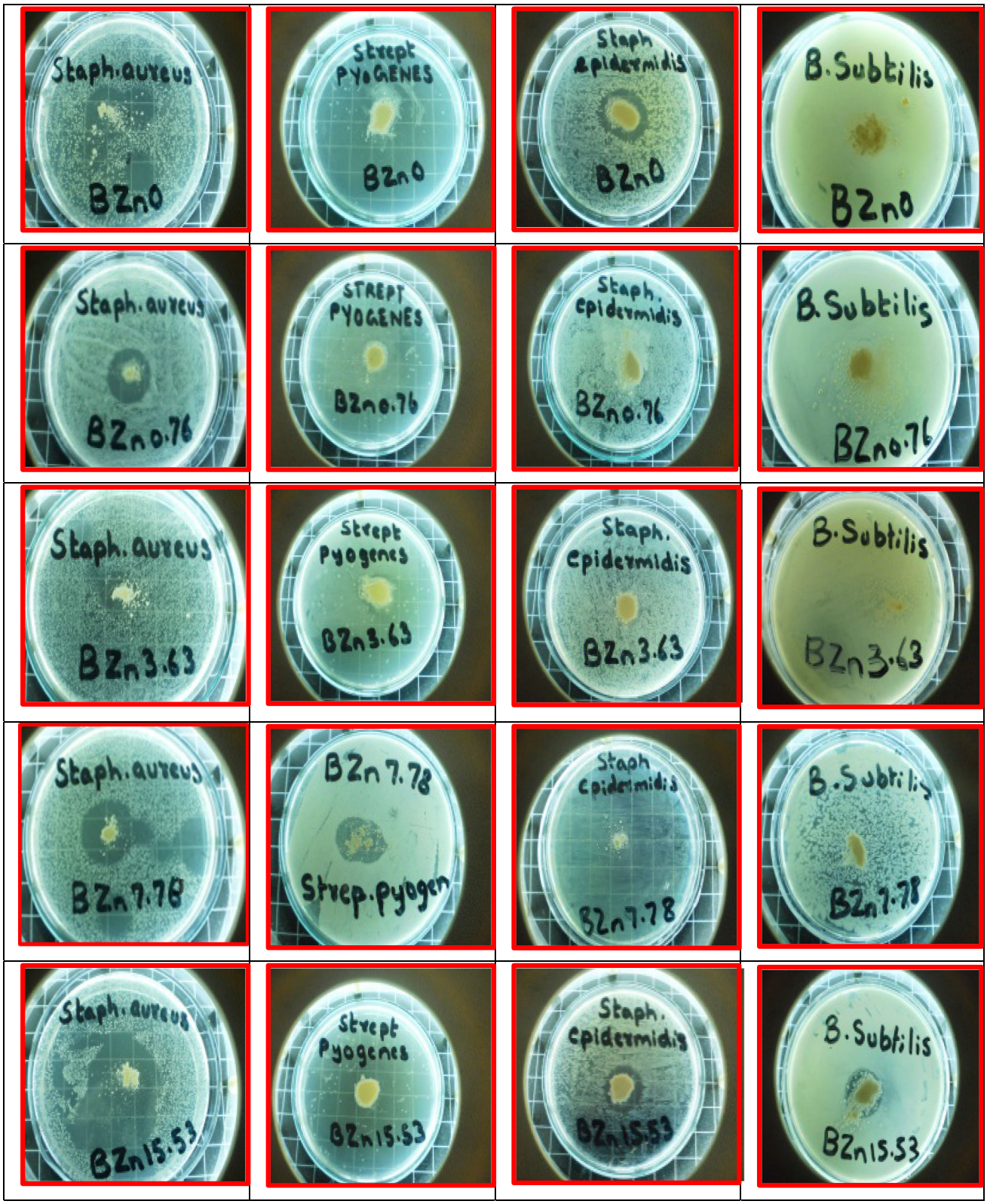

Fig. 6 Zone of inhibition produced by different glass–ceramics against gram-positive bacteria

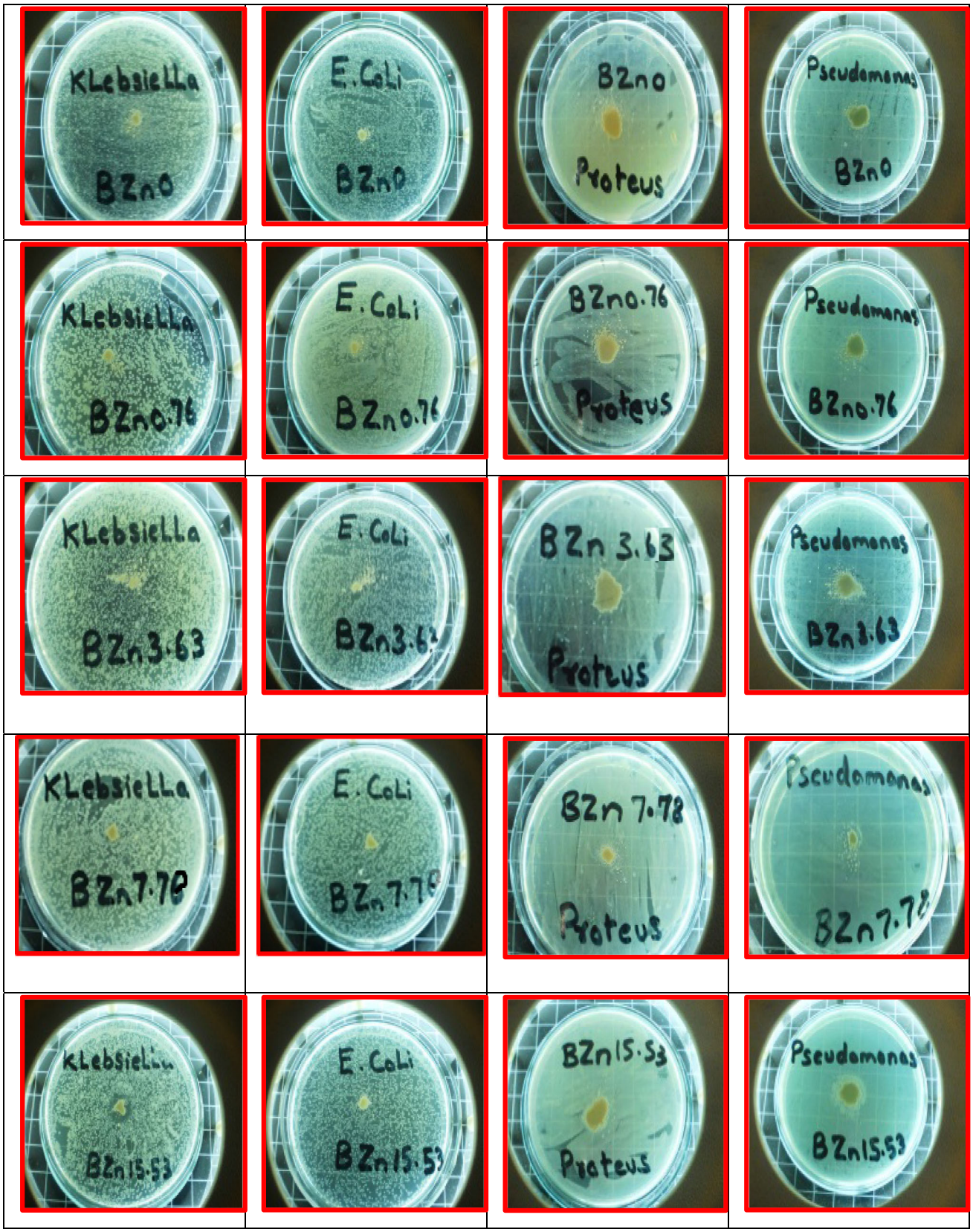

Fig. 7 Zone of inhibition produced by different glass–ceramics against gram-negative bacteria

Table 4 Pair wise mean comparison to specify significance level evaluated by one-way ANOVA test

	Mean comparison	Mean difference	*Significance
S. aureus	BZn0.76 BZn0	−6.53	1
	BZn3.63 BZn0	−13.32333	1
	BZn3.63 BZn0.76	−6.79333	1
	BZn7.78 BZn0	−3.69667	1
	BZn7.78 BZn0.76	2.83333	1
	BZn7.78 BZn3.63	9.62667	1
	BZn15.53 BZn0	13.33667	1
	BZn15.53 BZn0.76	19.86667	1
	BZn15.53 BZn3.63	26.66	1
	BZn15.53 BZn7.78	17.03333	1
S. pyogenes	BZn0.76 BZn0	−68.01	1
	BZn3.63 BZn0	−68.01	1
	BZn3.63 BZn0.76	0	0
	BZn7.78 BZn0	−47.8	1
	BZn7.78 BZn0.76	20.21	1
	BZn7.78 BZn3.63	20.21	1
	BZn15.53 BZn0	−7.87667	1
	BZn15.53 BZn0.76	60.13333	1
	BZn15.53 BZn3.63	60.13333	1
	BZn15.53 BZn7.78	39.92333	1
S. epidermidis	BZn0.76 BZn0	−21.33333	1
	BZn3.63 BZn0	−21.33333	1
	BZn3.63 BZn0.76	0	0
	BZn7.78 BZn0	−21.33333	1
	BZn7.78 BZn0.76	0	0
	BZn7.78 BZn3.63	0	0
	BZn15.53 BZn0	0.42	0
	BZn15.53 BZn0.76	21.75333	1
	BZn15.53 BZn3.63	21.75333	1
	BZn15.53 BZn7.78	21.75333	1
B. subtilis	BZn0.76 BZn0	0	0
	BZn3.63 BZn0	0	0
	BZn3.63 BZn0.76	0	0
	BZn7.78 BZn0	0	0
	BZn7.78 BZn0.76	0	0
	BZn7.78 BZn3.63	0	0
	BZn15.53 BZn0	12	1
	BZn15.53 BZn0.76	12	1
	BZn15.53 BZn3.63	12	1
	BZn15.53 BZn7.78	12	1
K. pneumonia	BZn0.76 BZn0	0	0
	BZn3.63 BZn0	0	0
	BZn3.63 BZn0.76	0	0
	BZn7.78 BZn0	0	0
	BZn7.78 BZn0.76	0	0
	BZn7.78 BZn3.63	0	0
	BZn15.53 BZn0	11.89	1
	BZn15.53 BZn0.76	11.89	1
	BZn15.53 BZn3.63	11.89	1
	BZn15.53 BZn7.78	11.89	1

* Significance equal to 1 indicates that the means difference is significant at the 0.05 level Significance equal to 0 indicates that the means difference is not significant at the 0.05 level

4 Conclusion

In the present study in vitro antibacterial activity of ZnO doped SiO_2–CaO–P_2O_5–Na_2O–CaF_2 glass–ceramics were studied against eight common pathogens. The specimens showed antibacterial activity against five bacteria; *Staph. aureus*, *Strep. Pyogenes, Staph. epidermidis*, *B. subtilis* and *Klebsiella pneumonia*. BZn15.53 had a statistically significant ($P < 0.05$) more potent effect on the studied microorganisms as compare to other test samples. There were two factors identified in the study that might be the possible reason for antibacterial resistance of BZn15.53, first is the release of Zn heavy metal ions that damage the respiratory system of cell by accumulating on the surface of cell and second the presence of hydroxyapatite phase in atomic lattice destroy the cell membrane by inducing reactive oxygen species that causes ultimately death of cell. BZn15.53 showed stronger and significant antibacterial effects against a wide selection of bacteria. The powdered glass–ceramics can be used as a coating for orthopedic prostheses to prevent bacterial growth.

Acknowledgments The authors acknowledge the Post Graduate Medical Institute (PGMI) Lahore, Pakistan for providing pure bacterial cultures.

References

1. Lin H, Zhang J, Qu F, Jiang J, Jiang P. In vitro hydroxyapatite-forming ability and antimicrobial properties of mesoporous bioactive glasses doped with Ti/Ag. J Nanomater. 2013; Article ID 786420, 1–8.
2. Bellantone M, Williams HD, Hench LL. Broad-spectrum bactericidal activity of Ag_2O-doped bioactive glass. Antimicrob Agents Chemother. 2002;46:1940–5.
3. Gristina AG. Biomaterial-centered infection: microbial adhesion versus tissue integration. Science. 1987;237:1588–95.
4. Balamurugan A, Balossier G, Laurent-Maquin D, Pina S, Rebelo AHS, Faure J, Ferreira JMF. An in vitro biological and antibacterial study on a sol–gel derived silver-incorporated bioglass system. Dent Mater. 2008;24:1343–51.
5. Díaz M, Barba F, Miranda M, Guitián F, Torrecillas R, Moya JS. Synthesis and antimicrobial activity of a silver-hydroxyapatite nanocomposite. J Nano Mat. 2009;14:1–6.
6. Ahmed AA, Ali AA, Mahmoud DAR, El-Fiqi AM. Preparation and characterization of antibacterial P_2O_5–CaO–Na_2O–Ag_2O glasses. J Biomed Mater Res Part A. 2011;98(1):132–42.
7. Mustaffa R, Yusof MR, Othman F, Rahmat A. Drug release study of porous hydroxyapatite coated gentamycin- as drug delivery system. Regen Res. 2012;1(2):61–7.
8. Gorriti M, Lopez JMP, Boccaccini AR, Audisio C, Gorustovich AA. In vitro study of the antibacterial activity of bioactive glass-ceramic scaffolds. Adv Eng Mater. 2009;11(7):67–70.
9. Zhang D, Munukka E, Hupa L, Ylänen H, Matti K. Factors controlling antibacterial properties of bioactive glasses. Key Eng Mater. 2007;330–332:173–6.
10. Allan I, Newman H, Wilson M. Antibacterial activity of particulate Bioglass® against supra- and subgingival bacteria. Key Eng Mater. 2001;22:1683–7.
11. Shirashi F, Toyada K, Fukinbara S. Photolytic Smf pfotocatalytic treatment of an aqueous solution containing microbial cells and organic compounds in an annular-flow reactor. Chem Eng Sci. 1999;54:1547–52.
12. Stefan R, Mihaela N, Spinu M, Popescu S. Antibacterial effect of ZnO-B_2O_3 Matrix Doped with Silver Ions on Gram Positive Bacteria Cultures. J Anim Sci Biotechnol. 2010;1:43.
13. Jafari A, Ghane M, Arastoo S. Synergistic antibacterial effects of nano zinc oxide combined with silver nanocrystales. Afr J Microbiol Res. 2011;5:5465–73.
14. Azam A, Ahmed AS, Oves M, Khan MS, Habib SS, Memic A. Antimicrobial activity of metal oxide nanoparticles against gram-positive and gram-negative bacteria: a comparative study. Int J Nanomed. 2012;7:6003–9.
15. Hench LL, Wilson J. An introduction to bioceramics, advanced series in ceramics, vol. 1. Singapore: World Scientific Publishing; 1993.
16. Kokubo T, Shigematsu M, Nagashima Y, Tashiro M, Nakamura T, Yamamuro T, Higashi S. Apatite- and wollastonite-containg glass-ceramics for prosthetic application. Bull Ins Chem Res. 1982;60(3–4):260–8.
17. Yoshimi T, Sugiyama N, Takeoka Y, Rikukawa M, Oribe K, Aizawa M. Changes of material properties of inorganic/organic hybrids fabricated by infiltration of poly(L-lactic acid) into open pores of porous hydroxyapatite ceramics in a simulated body fluid. J Aus Ceram Soc. 2011;47(1):18–22.
18. Kokubo T, Kitsugi T, Yamamuro T. Solution able to reproduce in vivo surface-structure changes in bioactive glass-ceramics A-W. J Biomed Mater Res. 1990;24:721–34.
19. Hench LL. Bioceramics: from concept to clinic. J Am Ceram Soc. 1991;74:1487–510.
20. Fujita H, Iida H, Ido K, Matsuda Y, Oka M, Nakamura T. Porous apatite-wollastonite glass-ceramic as an intramedullary plug. J Bone Joint Surg [Br]. 2000;82(4):614–8.
21. Salman SM, Salama SN, Darwish H, Abo-Mosallam HA. In vitro bioactivity of glass-ceramics of the $CaMgSi_2O_6$-$CaSiO_3$-$Ca_5(PO_4)_3F$-Na_2SiO_3 system with TiO_2 or ZnO additives. Ceram Int. 2009;35:1083–93.
22. Kamitakahara M, Ohtsuki C, Inada H, Tanihara M, Miyazaki T. Effect of ZnO addition on bioactive CaO–SiO_2–P_2O_5–CaF_2 glass-ceramics containing apatite and wollastonite. Acta Biomater. 2006;2:467–71.
23. Saino E, Grandi S, Quartarone E, Maliardi V, Galli D, Bloise N, Fassina L, Gabriella M, De Angelis C, Mustarelli P, Imbriani M, Visai L. In vitro calcified matrix deposition by human osteoblasts onto a zinc-containing bioactive glass. Eur Cell Mater. 2011;21:59–72.
24. Riaz M, Zia R, Saleemi F, Bashir F, Hossain T, Kayani Z. In vitro evaluation of bioactivity of SiO_2–CaO–P_2O_5–Na_2O–CaF_2–ZnO glass-ceramics. Mat Sci Poland. 2014;32(3):364–74.
25. Hench LL. The story of bioglass. J Mat Sci. 2006;17(11):967–78.
26. Zia R, Riaz M, Maqsood S, Anjum S, Kayani Z, Hussain T. Titania doped bioactive ceramics prepared by solid state sintering method. Ceram Int. 2015;41:8964–72.
27. Sawi J. Quantitative evaluation of antibacterial activities of metallic oxide powders (ZnO, MgO and CaO) by conductimetric assay. J Microbiol Methods. 2003;54:177–82.
28. Sevinç BA, Hanley L. Antibacterial activity of dental composites containing zinc oxide nanoparticles. J Biomed Mater Res Part B. 2010;94:22–31.
29. Kokubo T, Shigematsu M, Nagashisma Y, Tashiro M, Nakamura T, Yamamuro T, Higashi S. Apatite- and wallostonite-containing

glass-ceramics for prosthetic application. Bull Inst Chem Res. 1982;60(3–4):260–8.
30. Jones N, Ray B, Ranjit KT, Manna AC. Antibacterial activity of ZnO nanoparticles suspensions on a broad spectrum of microorganisms. FEMS Microbiol Lett. 2008;279:71–6.
31. Premanthan M, Karthikeyan K, Jeyasubramanian K, Manivannam G. Selective toxicity of ZnO nanoparticles towards Gram-positive bacteria and cancer cells by apoptosis through lipid peroxidation. Nanomedicine. 2011;7:184–92.
32. Bauer AW, Kirby WMH, Sherris JC, Trunk M. Antibioatic succeptability testing by a standardized single disc method. Am J Clin Pathol. 1966;45:493–6.
33. Kokubo T, Takadama H. How useful is SBF in predicting in vivo bone bioactivity? Biomaterials. 2006;27(15):2907–15.
34. Deepa C, Begum AN, Aravindan S. Preparation and antimicrobial observations of zinc doped nanohydroxyapatite. Nanosist FiZ Himmat. 2013;4(3):370–7.
35. Driscoll AJ, Bhat N, Karron RA, O'Brien KL, Murdoch DR. Disk diffusion bioassays for the detection of antibiotic activity in body fluids: applications for the pneumonia etiology research for child health project. Clin Infect Dis. 2012;54(S2):159–64.
36. Stoor P, Soderling E, Salonen JI. Antibacterial effects of a bioactive glass paste on oral microorganisms. Acta Odontol Scand. 1998;56:161–5.
37. Stoor P, Soderling E, Grenman R. Interations between bioactive glass S53P4 and the atrophic rhinitis-associated microoganism *klebsiella ozaenae*. J Biomed Mater Res B Appl Biomater. 1999;48:869–74.
38. Zehnder M, Baumgartner G, Marquardt K, Paque F. Prevention of bacterial leakage through instrumented root canals by bioactive glass S53P4 and calcium hydroxide suspension in vitro. Oral Surg Oral Med Oral Pathol Oral Radiol Endod. 2007;103:423–8.
39. Jesline A, John NP, Narayanan PM, Vani C, Murugan S. Antimicrobial activity of zinc and titanium dioxide nanoparticles against biofilm-producing methicillin-resistant Staphylococcus aureus. Appl Nanosci. 2015;5:157–62.
40. Nies DH. Microbial heavy-metal resistance. Appl Microbiol Biotechnol. 1999;51(6):730–50.
41. Hu S, Chang J, Liu M, Ning C. Study on antibacterial effect of 45S5 Bioglass. J Mater Sci Mater Med. 2009;20(1):281–6.
42. Adwan K, Abu-Hasan N. Gentamicin resistance in clinical strains of Enterobacteriaceae associated with reduced gentamicin uptake. Folia Microbiol. 1998;43:438–40.